

■ Host–Guest Systems

A Supramolecular Vesicle Based on the Complexation of *p*-Sulfonatocalixarene with Protamine and its Trypsin-Triggered Controllable-Release Properties

Kui Wang,^[a, b] Dong-Sheng Guo,^[a] Meng-Yao Zhao,^[a] and Yu Liu^{*[a]}

Abstract: Enzyme-responsive assembly represents one of the increasingly significant topics in biomaterials research and finds feasible applications to the controlled release of therapeutic agents at specific sites at which the target enzymes are located. In this work, based on the concept of host–guest chemistry, a trypsin-responsive supramolecular vesicle using *p*-sulfonatocalix[4]arene as the macrocyclic

host and natural serine protease trypsin-cleavable cationic protein protamine as the guest molecule, is reported. The complexation of *p*-sulfonatocalix[4]arene with protamine directs the formation of a supramolecular binary vesicle, which is dissipated by trypsin with high selectivity. Therefore, the present system represents a principle-of-concept to build a controlled-release carrier at trypsin-overexpressed sites.

Introduction

Stimuli-responsive amphiphiles have developed greatly in recent years as a result of their prospective uses in the fields of chemistry, biology, and material science, in which drug/gene delivery systems have gained foremost attention because their controlled-release characteristics have resulted in enhanced efficacy at the site of action.^[1–7] Enzymes play essential roles in most biochemical processes, and the abnormal activity of enzymes has always been associated with many diseases.^[8–11] As an appealing quest for therapeutic purposes, comparing with other stimuli, such as temperature, pH, and light, enzyme-responsive amphiphilic assemblies have captured much more attention in many biological fields,^[12–14] in which the loaded drugs can be released from self-assembled vehicles triggered by specific enzymatic reactions at the enzyme-overexpressed sites with good biocompatibility, high degree of sensitivity, and selectivity.^[15–19] However, introducing enzyme-responsive sites into amphiphiles generally requires a tedious and time-consuming covalent synthesis, thus not only raising the cost of preparation as well as reducing their biocompatibility but also affecting the efficacy due to suboptimal reactivity of the

enzyme to the modified substrates. In this regard, a supramolecular approach paves a smart, alternative way to build enzyme-responsive amphiphilic assemblies, in which enzyme-responsive moieties can be grafted into amphiphiles by reversible non-covalent interactions. However, it is unsatisfying that the concept of “supra-amphiphiles”^[20–22] is by far less travelled in building enzyme-responsive supramolecular amphiphilic assemblies^[23–27] due to the challenge of screening for a suitable enzyme-responsive building block, especially for building an enzyme-responsive supramolecular vesicle.^[28]

Up to now, several kinds of non-covalent interactions have been used to tune the molecular amphiphilicity and self-assembled nanostructures, including hydrogen-bonding, charge-transfer, and $\pi\cdots\pi$ interactions, among others.^[20–22] These non-covalent interactions often employed are not always effective for designing supra-amphiphiles in water, and therefore, they lack the necessary biocompatibility for applications in the field of biotechnology. Macrocyclic receptors, such as cyclodextrin, sulfonatocalixarene, and cucurbituril, are all water-soluble and exhibit particular advantages in building water-soluble supramolecular assemblies.^[29–32] For example, Tian and Li et al. recently constructed a light-driven, linear, chiral supramolecular polymer in water using both sulfonatocalixarene and cyclodextrin.^[33] Moreover, these three macrocyclic species have been confirmed to be biocompatible.^[34–37] Consequently, fabricating supra-amphiphiles through host–guest complexation is of particular interest and importance in the fields of biotechnology and pharmaceuticals. However, to the best of our knowledge, supramolecular vesicles formed by host–guest interactions between macrocyclic hosts and guests have been underexplored.^[38, 39]

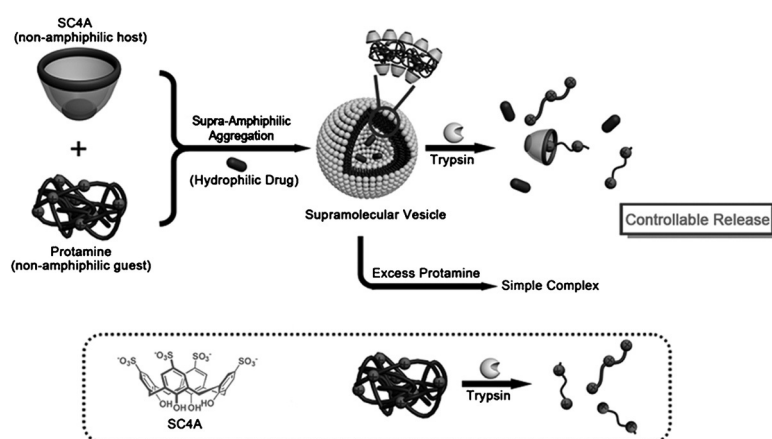
We present here a feasible strategy for building serine protease trypsin-responsive supramolecular vesicles in water as a controllable release model at trypsin-overexpressed sites upon host–guest complexation employing biocompatible *p*-

[a] Dr. K. Wang, Dr. D.-S. Guo, M.-Y. Zhao, Prof. Dr. Y. Liu
Department of Chemistry
State Key Laboratory of Elemento–Organic Chemistry
Nankai University, Tianjin 300071 (P.R. China)
E-mail: yuliu@nankai.edu.cn

[b] Dr. K. Wang
Tianjin Key Laboratory of Structure and
Performance for Functional Molecules
Key Laboratory of Inorganic–Organic Hybrid
Functional Material Chemistry, Ministry of Education
College of Chemistry, Tianjin Normal University
Tianjin 300387 (P.R. China)

Supporting information for this article is available on the WWW under
<http://dx.doi.org/10.1002/chem.201303963>.

sulfonatocalix[4]arene (SC4A)^[34,35] as the macrocyclic host and natural biological cationic protein protamine as the enzyme-cleavable guest (avoiding the tedious covalent syntheses and substrate modification), respectively. The design proposed herein combines the following four advantages: 1) both of the two components are biocompatible; 2) differing from the sulfonatocalixarene-based supramolecular vesicles formed by sulfonatocalixarene-induced small amphiphilic cationic guest aggregations upon host-guest complexation,^[28,40–45] the guest employed here to construct sulfonatocalixarene-based supramolecular vesicle is a completely non-amphiphilic natural biological cationic protein, utilizing a new principle of guest-guided sulfonatocalixarene amphiphilic aggregation upon host-guest complexation, which would greatly expand the range of engaging substrates (especially natural biological molecules) in fabricating enzyme-responsive supra-amphiphiles; 3) trypsin converts protamine to amino acid and peptide with unparalleled specificity upon progressive cleavage of peptide bonds in the protein; 4) the cleavage of peptide bonds in the protein leads to the complexed vesicle dissipated (Scheme 1). In fact, many studies have been focused on the interactions between sulfonatocalixarene and proteins because the struc-



Scheme 1. Schematic illustration of the supra-amphiphilic assembly of SC4A with protamine and its trypsin-triggered controllable release.

tural characterization of protein surface–ligand complexes is a necessary step towards the development of new methods of non-covalent modification. However, all the reported interactions between sulfonatocalixarene and proteins only lead to the formation of simple inclusion complexes. Well-defined functional assembly formed by the complexation of sulfonatocalixarene with protein has not been reported by far. On the other hand, the present work represents the first example of trypsin-responsive vesicle, which is constructed by using a host-guest strategy. Therefore, the present system is conceptually applicable as a controllable-release model at trypsin-overexpressed sites.^[46–48]

Results and Discussion

Construction of supramolecular binary vesicles

Although protamine is a natural trypsin-responsive biological cationic protein, it is unable to fabricate trypsin-responsive amphiphilic assembly independently due to its high hydrophilic property, in which as high as two thirds of its amino acids are positively charged residues. Excitingly, benefiting from the strong binding affinity of anionic SC4A toward organic cations,^[49,50] a simple mixture of SC4A (0.02 mM) and protamine (50 $\mu\text{g mL}^{-1}$) in aqueous solution shows the Tyndall effect, which prompted us to explore the higher hierarchy assembly based on the host-guest complexation of SC4A with protamine. The critical aggregation concentration (CAC) of SC4A in the presence of 50 $\mu\text{g mL}^{-1}$ of protamine was measured by monitoring the dependence of the optical transmittance around 450 nm on the concentration of SC4A. Upon addition of protamine, the optical transmittance decreases gradually with increasing SC4A concentration as a result of amphiphilic assembly (Figure 1a). The complexation-induced CAC value of 0.01 mM can therefore be obtained according to the plot of optical transmittance at 450 nm versus concentration of SC4A (Figure 1b). It is noted that in the absence of protamine, SC4A is without any tendency to self-aggregation in aqueous solution.^[51]

It is a prerequisite to determine the preferable mixing ratio between SC4A and protamine for fabricating the binary amphiphilic assembly. Figure 2 shows the optical transmittance spectra (a) and the plot of transmittance at 450 nm as a function of the concentration of protamine added to a SC4A solution at fixed 0.02 mM (b). The transmittance at 450 nm first decreased sharply with increasing protamine concentration until the minimum was reached at 50 $\mu\text{g mL}^{-1}$ of protamine and then gradually increased thereafter to approach a quasi-plateau. In the left-hand portion of inflection, SC4A and protamine form a higher-order complex with a tendency toward amphiphilic assembly, whereas in the right-hand portion of inflection, excess protamine leads to the formation of simple inclusion complex accompanied by the disassembly of the amphiphilic assembly. The inflection means that, in the present SC4A–protamine system, the preferable mixing ratio for the amphiphilic assembly is 50 $\mu\text{g mL}^{-1}$ protamine/0.02 mM SC4A. Control experiments show that neither replacement of SC4A by its building subunit 4-phenolsulfonic sodium nor replacement of protamine by its main composition arginine could induce the formation of assembly (see the Supporting Information, Figure S1), indicating that the conical

amphiphilic assembly. The inflection means that, in the present SC4A–protamine system, the preferable mixing ratio for the amphiphilic assembly is 50 $\mu\text{g mL}^{-1}$ protamine/0.02 mM SC4A. Control experiments show that neither replacement of SC4A by its building subunit 4-phenolsulfonic sodium nor replacement of protamine by its main composition arginine could induce the formation of assembly (see the Supporting Information, Figure S1), indicating that the conical

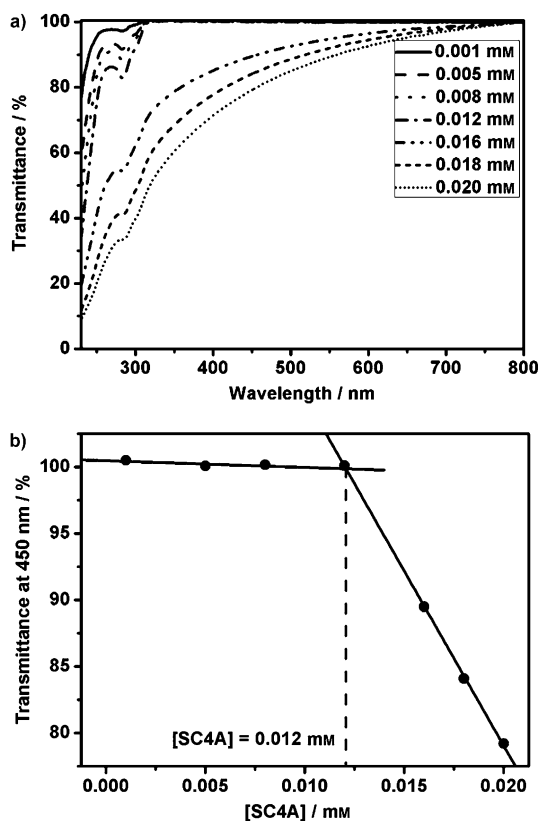


Figure 1. a) Optical transmittance of aqueous solutions of SC4A at different concentrations in the presence of protamine ($50 \mu\text{g mL}^{-1}$) at 25°C . b) Dependence of the optical transmittance at 450 nm on SC4A concentration in the presence of protamine ($50 \mu\text{g mL}^{-1}$).

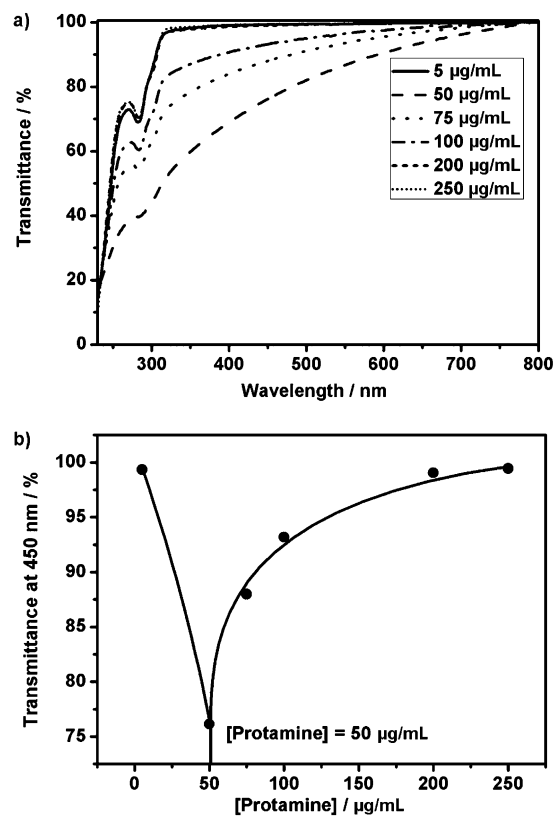


Figure 2. a) Optical transmittance of SC4A (0.02 mM) by increasing the concentration of protamine from 5 to $250 \mu\text{g mL}^{-1}$ at 25°C in water. b) Dependence of the optical transmittance at 450 nm on the protamine concentration with a fixed SC4A concentration of 0.02 mM .

cavity of SC4A and the polycationic structure of protamine are the crucial factors leading to SC4A–protamine amphiphilic assembly.

The solution of SC4–protamine exhibited a clear Tyndall effect (Figure 3a), indicating the existence of abundant nanoparticles. However, neither free SC4A or protamine solution nor protamine-4-phenolsulfonic sodium or SC4A–arginine solution exhibited the similar Tyndall effect, revealing that neither only free SC4A nor protamine can form nanoscale aggregates under the same conditions, but also neither replacement of SC4A by its building subunit 4-phenolsulfonic sodium nor replacement of protamine by its main composition arginine can induce the formation of nanoscale aggregates, which is in accordance with the above optical transmittance results. Furthermore, dynamic laser scattering (DLS), scanning electron microscopy (SEM), and transmission electron microscopy (TEM) were employed to identify the self-assembled size and morphology of SC4A–protamine supra-amphiphilic assembly. DLS result shows that the SC4A–protamine complex forms well-defined aggregates with a narrow size distribution, giving an average diameter of 395 nm at a scattering angle of 90° (Figure 3b). The SEM image (Figure 3c) shows the spherical morphology with an average diameter of about 250 nm. The measured diameters of the aggregates exceed the corresponding extended molecular length, suggesting that these aggregates are vesicular entities rather than simple micelles.^[52] The formation of

vesicles was convincingly validated by cryo-TEM image (Figure 3d) as well as high-resolution TEM image (Figure 3e), showing the hollow spherical morphology. From the distinguishably dark periphery and the light central parts, we obtained the thickness of the bilayer membrane as about 3.5 nm. Zeta potential measurement was further performed to identify the SC4A–protamine vesicular surface charged distribution, giving an average zeta potential of $+17.32 \text{ mV}$ (see the Supporting Information, Figure S2), which is in accordance with the positively charged property of the resulting SC4A (0.02 mM)/protamine ($50 \mu\text{g mL}^{-1}$) vesicle in theory.

Combining all the aforementioned results, we may deduce two possible modes of forming SC4A–protamine supramolecular vesicles (see the Supporting Information, Scheme S1). The arrangement B (The inner- and outer-layer surfaces consist of hydrophilic phenol OH groups of SC4A, which are exposed to the aqueous solution, and SC4A and protamine are connected together by host–guest interactions.) seems to be most favorable because a precipitate would be found if we replaced SC4A by ethyl-modified SC4A at OH groups to construct supramolecular vesicles with protamine under the same conditions. Until now, building sulfonatocalixarene-based supramolecular vesicles is limited to the complexation of sulfonatocalixarene with small amphiphilic cationic guests, utilizing the principle of calixarene-induced guest aggregation.^[28,40–45] However, the guest employed here to construct sulfonatocalixarene-based supra-

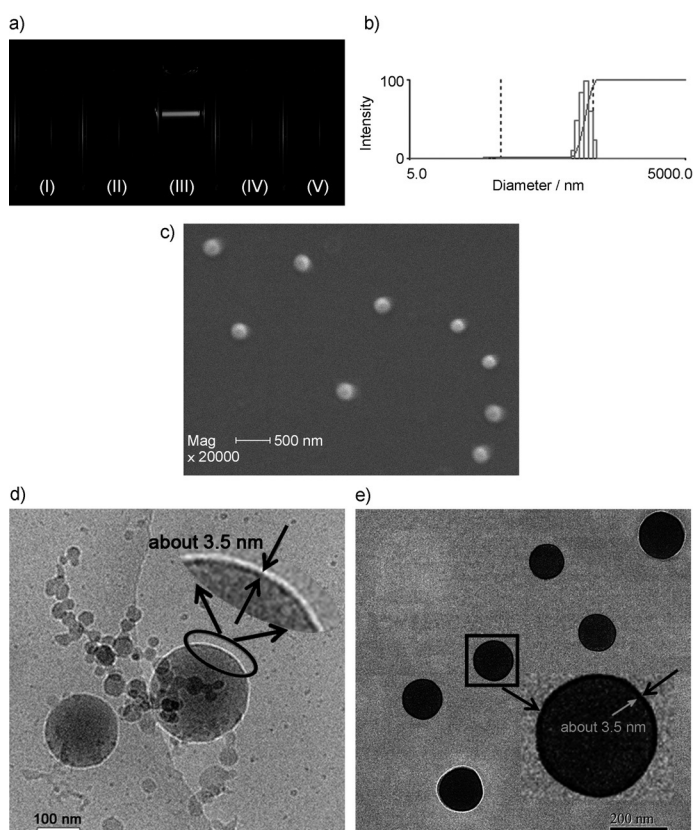


Figure 3. a) Tyndall effect of free SC4A (I), free protamine (II), SC4A–protamine (III), protamine-4-phenolsulfonic sodium (IV), and SC4A–arginine (V). b) DLS data of the SC4A–protamine assembly; c) SEM, d) cryo-TEM, and e) high-resolution TEM images of the SC4A–protamine assembly. [SC4A] = 0.02 mM, [protamine] = 50 $\mu\text{g mL}^{-1}$, [4-phenolsulfonic sodium] = 0.08 mM, and [arginine] = 0.25 mM.

molecular vesicle is a completely non-amphiphilic natural biological cationic protein, utilizing a new principle of guest-guided sulfonatocalixarene amphiphilic aggregation upon host–guest complexation. This new finding not only enriches the research area of supramolecular vesicles based on calixarenes but also helps us to understand the essence of building sulfonatocalixarene-based supramolecular vesicles. Intrinsically, the complexation of negatively charged sulfonatocalixarene with positively charged guests compensates the original charge repulsion that is unfavorable for amphiphilic aggregation of free components. Three key factors are generally demanded: 1) benefiting from the synergistic effect of calixarene cavities and additional anchoring points donated by sulfonate groups, sulfonatocalixarenes are capable of forming higher-order complexes with tailored guests; 2) the preorganized conical framework of calixarenes contributing to curvature aggregation and enhanced stability of amphiphilic aggregation, and their lower-rim hydrophilic OH groups toward aqueous solution are also requisite; 3) the suitable cationic guest could be either a small amphiphilic cation that can be induced to aggregate by the complexation of sulfonatocalixarene reported before,^[28,40–45] or a covalent non-amphiphilic polycationic guest that can guide sulfonatocalixarene amphiphilic aggregation by host–guest complexation, like protamine used here.

Trypsin-response of the SC4A–protamine vesicles

The disassembly process induced by trypsin was firstly monitored by optical transmittance. We were gratified to find a considerable increase in the optical transmittance after adding trypsin to the SC4A–protamine solution, which reached about 95% at 450 nm after 5 h (Figure 4a), indicating that most vesicular assemblies disappeared in about 5 h. More powerful evidence for the disassembly of the vesicles upon addition of trypsin comes from DLS measurements, showing that the scattering intensity decreases pronouncedly from several Mcps to tens of kcps under the same conditions in 5 h, accompanied by the almost disappearance of turbidity and Tyndall effect (Figure 4b). High-resolution TEM (Figure 4c) and SEM (Figure 4d) images also show that hardly any vesicular morphology was observed after trypsin treatment. The rate for the trypsin-responsive disassembly is related to the concentration of the enzyme added (see the Supporting Information, Figure S3), and the hydrolysis rate of the binary vesicle by trypsin is much slower than the hydrolysis rate of free protamine by trypsin because there is a dynamic equilibrium between the assembled and unassembled states of protamine, and trypsin attacks only the free species. Control experiments show that there was no significant change in either the optical transmittance at 450 nm or the turbidity and Tyndall effect without adding trypsin to the SC4A–protamine solution over the same time range (see the Supporting Information, Figure S4), indicating that SC4A–protamine binary vesicles are stable at room temperature. We further studied the stability and trypsin responsiveness of formed nanoparticles in normal saline (high salt concentration; 0.9% w/v NaCl). Compared with the nanoparticle solution with trypsin, we found that there was only a little change over the same time range in the optical transmittance at 450 nm for the nanoparticle solution without trypsin (see the Supporting Information, Figure S5a). On the other hand, the turbidity and Tyndall effect for the nanoparticle solution with trypsin almost disappeared in 5 h, however, there was no significant change in turbidity and Tyndall effect for the nanoparticle solution without trypsin over the same time range (see the Supporting Information, Figure S5b). Both of them indicated that although high salt concentrations would affect the stability of formed nanoparticles seriously compared with pure water, SC4A–protamine binary vesicles can still exist in normal saline and be disassembled by trypsin hydrolysis.

To prove that the activity of trypsin is the crucial factor contributing to the disassembly of the vesicles, a control experiment was carried out in which the same amount of denatured trypsin (treated in boiling water for 1 h) was added to the SC4A–protamine solution. The results show that no appreciable change over time was observed in either the optical transmittance at 450 nm or the turbidity and Tyndall effect (see the Supporting Information, Figure S6), thus clearly indicating that

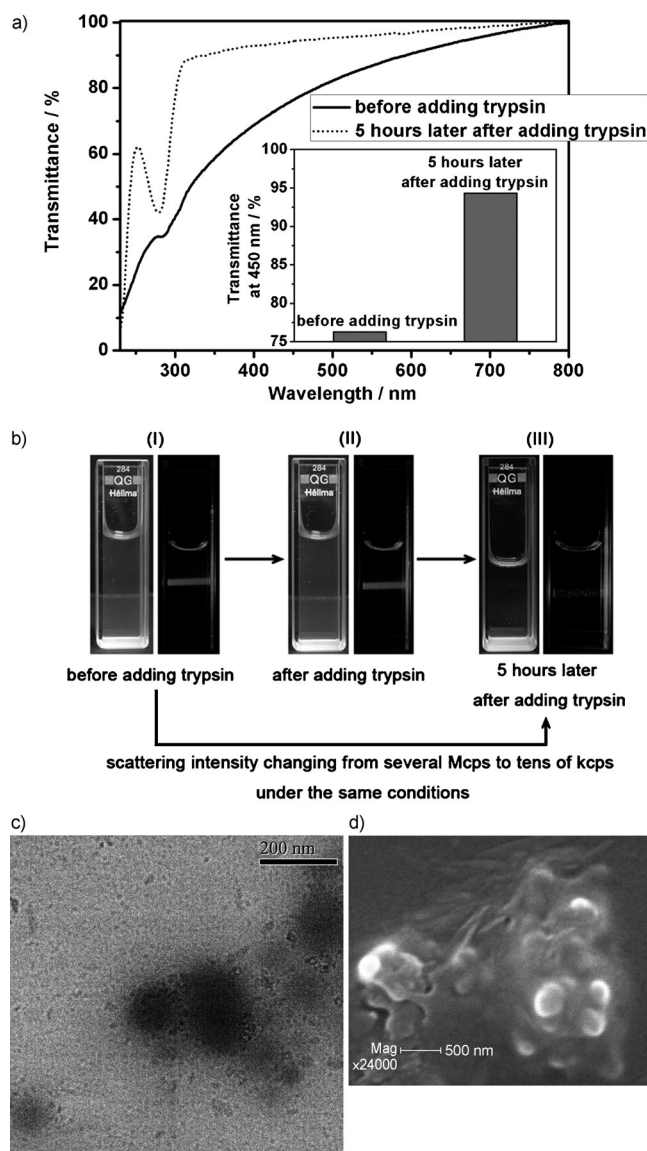


Figure 4. a) Optical transmittance of SC4A–protamine assembly before and after addition of trypsin for 5 h in water. Inset: comparison of the optical transmittance at 450 nm. b) Turbidity and Tyndall effect of SC4A–protamine assembly before (I) and immediately after addition of trypsin (II), and after addition of trypsin for 5 h (III) in water. c) High-resolution TEM, and d) SEM images of the SC4A–protamine assembly after addition of trypsin for 5 h. [SC4A] = 0.02 mM, [protamine] = 50 $\mu\text{g mL}^{-1}$, and [trypsin] = 0.2 mg mL^{-1} .

the disassembly of the SC4A–protamine vesicles depends on the cleavage of peptide bonds in the protein by trypsin. To investigate the specificity of the trypsin-responsive disassembly, the optical transmittance results for the SC4A–protamine solution upon addition of other kinds of enzymes such as calf intestinal alkaline phosphatase (CIAP), exonuclease I (Exo I), and glucose oxidase (GOx) were recorded. As shown in Figure S7 (the Supporting Information), in the presence of CIAP/Exo I/GOx, there was no significant change over time in either the optical transmittance at 450 nm or the turbidity and Tyndall effect, demonstrating that this enzyme-responsive vesicle exhibits excellent specificity toward trypsin. We further used some other proteases as controls. As shown in Figure S8 (the

Supporting Information), in the presence of proteinase K/ α -chymotrypsin, there was also no significant change in either the optical transmittance at 450 nm or the turbidity and Tyndall effect over the same time range, demonstrating undoubtedly that although other proteases may also cleave protamine, their efficiencies are quite lower than the efficiency of trypsin.

Loading model molecules by the vesicles and its trypsin-triggered controllable-release properties

It is reasonable to expect that the trypsin-responsive disassembly would trigger a concomitant release of any hydrophilic molecule sequestered within the vesicular interior. To test this, the trisodium salt of 8-hydroxypyrene-1,3,6-trisulfonic acid (HPTS) as a model molecule was loaded into the vesicles. DLS experiment for protamine–HPTS mixture as a control showed no signal (see the Supporting Information, Figure S9), which indicated that protamine and negatively charged small molecule could not form nanoparticles well. The release kinetics of HPTS with and without addition of trypsin was studied through fluorescence emission spectroscopy (see the Supporting Information, Figure S10). As shown in Figure 5, a very low release of entrapped HPTS was observed over periods of 5 h, indicating

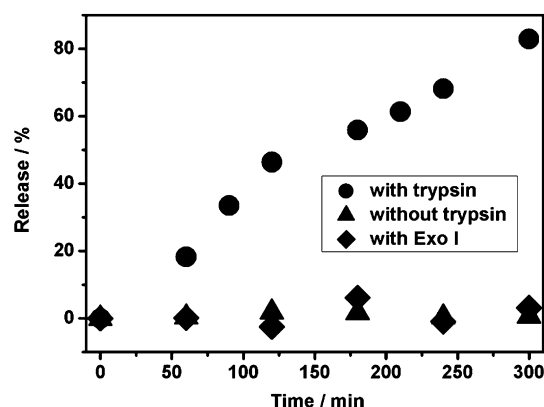


Figure 5. Release of HPTS entrapped in the supramolecular SC4A–protamine vesicle with and without trypsin, as well as with Exo I. [SC4A] = 0.02 mM, [protamine] = 50 $\mu\text{g mL}^{-1}$, [trypsin] = 0.2 mg mL^{-1} , and [Exo I] = 0.5 U mL^{-1} .

that the vesicles are highly stable toward leakage at room temperature in aqueous medium. However, the release rate was significantly enhanced when the vesicles were treated with trypsin, and more than 80% HPTS had been released in 5 h, demonstrating the efficient trypsin-triggered disassembly and release of the SC4A–protamine binary vesicles. In addition, there was almost no HPTS release observed for the vesicle solution treated with other enzymes such as Exo I, as expected. These phenomena imply that the present system is conceptually applicable as a controllable-release model, which encapsulate hydrophilic model molecules inside and release them when encountered with trypsin, in particular at the sites at which trypsin is overexpressed.

Basic cell experiments were further carried out to evaluate the cellular toxicity of the supramolecular binary vesicle and

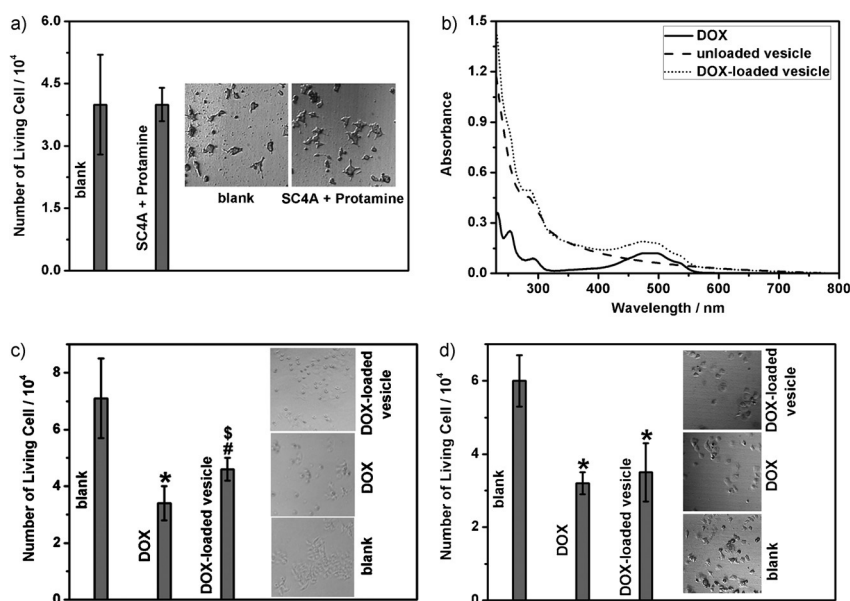


Figure 6. a) Number of living NIT-1 cells in the blank group and after treatment with SC4A–protamine vesicle for 24 h. Inset: images of living NIT-1 cells in the blank and SC4A–protamine vesicle groups after 24 h. b) UV/Vis absorption spectra of DOX, the unloaded vesicle, and DOX-loaded vesicle at 25 °C in water. c) Number of living HepG-2 cells in the blank group and after treatment with bare DOX and DOX-loaded vesicle for 24 h. Inset: images of living HepG-2 cells in the blank, DOX, and DOX-loaded vesicle groups after 24 h. The asterisk indicates $P < 0.01$ versus the blank group, number sign (#) indicates $P < 0.05$ versus the blank group, and the dollar sign indicates $P < 0.05$ versus the DOX group. d) Number of living PANC-1 cells in the blank group and after treatment with bare DOX and DOX-loaded vesicle for 24 h. Inset: images of living PANC-1 cells in the blank, DOX, and DOX-loaded vesicle groups after 24 h. The asterisks indicate $P < 0.01$ versus the blank group.

study its trypsin-triggered controllable-release properties in vitro. First, NIT-1 cells (pancreatic islet beta cells in mice) were incubated with and without SC4A–protamine vesicle, and the number of living cells in each group was recorded after 24 h. As shown in Figure 6a, we found that the number of living NIT-1 cells in the vesicle group was statistically equivalent to that in the blank group ($P > 0.05$) and the morphology of living cells in the vesicle group was also similar to that in the blank group. All these results suggest that the SC4A–protamine vesicle employed in this work is practically non-toxic and therefore is an ideal controllable-release carrier, which is in accordance with the biocompatible property of individual SC4A and protamine. Next, we loaded doxorubicin hydrochloride (DOX), a typical hydrophilic broad-spectrum anticancer drug, into the SC4A–protamine vesicle. In comparison with the unloaded one, the absorption of the loaded vesicle becomes much stronger from 450 to 550 nm (Figure 6b), which represents the characteristic absorption of DOX. Moreover, the vesicular solution turns from colorless to light-red (see the Supporting Information, Figure S11). Both of them confirm undoubtedly that DOX was successfully loaded in the inner cavity of vesicle. According to UV/Vis absorption spectra, the DOX loading efficiency was calculated to be 8.3%. Then HepG-2 cells (hepatic carcinoma cells in human) and PANC-1 cells (pancreatic carcinoma cells in human) were incubated with and without bare DOX and DOX-loaded vesicle, respectively, and the number of living cells in each group was also recorded after 24 h. As shown in Figure 6c, we found that the number of living HepG-2 cells in

the DOX group was much less than that in the blank group ($P < 0.01$), which showed the efficient therapeutic effect of DOX for hepatic carcinoma cells. However, the number of living HepG-2 cells in the DOX-loaded vesicle group was only a little less than that in the blank group ($P < 0.05$), and we also found that the number of living HepG-2 cells in the DOX-loaded vesicle group was statistically more than that in the DOX group ($P < 0.05$), both of which implied that the therapeutic effect of loaded-DOX by this vesicle for hepatic carcinoma cells was reduced due to the protection of DOX in the inner cavity of vesicle, although the anticancer drug DOX has a stronger interaction with cancer cells.^[41] Differing from HepG-2 cells, we excitingly found that the numbers of living PANC-1 cells in both the DOX group and the DOX-loaded vesicle group were much less than that in the blank group ($P < 0.01$;

Figure 6d). Furthermore, no obvious differences were observed for both the number ($P > 0.05$) and the morphology of living PANC-1 cells in the DOX and DOX-loaded vesicle groups. Both of them indicate that the loading of DOX by SC4A–protamine vesicle does not affect the therapeutic effect of DOX for pancreatic carcinoma cells. One reasonable explanation is the trypsin-triggered disassembly of the SC4A–protamine vesicle and then release of loaded-DOX due to the overexpression of trypsin in pancreatic carcinoma cells. Compared with bare DOX, the discrepant therapeutic effect of loaded-DOX by SC4A–protamine vesicle for hepatic carcinoma cells and pancreatic carcinoma cells reveals the potential trypsin-triggered controllable release of SC4A–protamine vesicle at trypsin-overexpressed sites in vitro. Fluorescence microscopy was further employed to monitor if the assemblies can be taken up by PANC-1 cells. As shown in Figure S12 (the Supporting Information), after a 24 h incubation of the PANC-1 cells with the HPTS-loaded vesicles, the green fluorescence of HPTS was monitored in the cells, demonstrating that SC4A–protamine vesicles can be taken up by PANC-1 cells. According to the size of the vesicle, the possible mechanism of uptake is deduced as endocytosis.

Finally, fluorescence imaging of mice was carried out to study the trypsin-triggered controllable release of the SC4A–protamine vesicle in vivo preliminarily. Fluorescein sodium was loaded in the inner cavity of vesicle and used as the probe here. After intraperitoneal injection of bare fluorescein and fluorescein-loaded vesicle in the pancreatic tissue of mice, respectively, the mice were imaged using a fluorescence-imaging

system. As shown in Figure S13 (the Supporting Information), compared with the mouse injected with fluorescein-loaded vesicles, we firstly qualitatively found that the fluorescent distribution in the mouse body that was injected with bare fluorescein was much more scattered at the same tested time-point post-injection, which possibly implied that the diffusion rate of bare fluorescein from pancreatic tissue to other parts of the body was much faster. Next, we quantitatively analyzed the relative fluorescence intensities at different parts of the bodies for the mice injected with bare fluorescein and fluorescein-loaded vesicles, respectively. We found that the relative fluorescence intensities (the fluorescence intensity around pancreatic tissue (part A) was normalized.) at almost all other parts for the mouse injected with bare fluorescein were stronger than the relative fluorescence intensities at the same parts for the mouse injected with fluorescein-loaded vesicles, such as 0.93/0.41 at part B, 0.55/0.40 at part C, and 0.57/0.41 at part D. The slowed diffusion rate of loaded-fluorescein from pancreatic tissue to other parts of the body implies the potential trypsin-triggered controllable release of the SC4A-protamine vesicles at the sites with abundant trypsin *in vivo*, such as pancreatic tissue exemplified here.

Conclusion

We have successfully constructed a trypsin-responsive supramolecular vesicle with high selectivity upon host-guest complexation employing biocompatible SC4A as the macrocyclic host and non-amphiphilic natural biological cationic protein protamine as the enzyme-cleavable guest, utilizing a new principle of guest-guided sulfonatocalixarene amphiphilic aggregation. A trypsin-induced cleavage of protamine triggers a cascade of events, loss of the hydrophilic-hydrophobic balance of the supramolecular binary vesicle, disassembly of the vesicle, and tandem release of entrapped hydrophilic model molecules. These findings not only help us to understand the essence of forming sulfonatocalixarene-based supramolecular vesicles, and as a result, greatly expand the range of substrate selection to fabricate enzyme-responsive supra-amphiphilic assemblies, but also show the charm of supramolecular chemistry that two or more components can self-assemble into higher-order structures, which exhibit unique properties and functions that the individual component cannot achieve. Furthermore, basic cell experiments and preliminary fluorescence imaging in mice imply that the present SC4A-protamine vesicle is conceptually applicable as a controllable-release model at trypsin-overexpressed sites. Such a trypsin-triggered controllable-release model is reasonably promising to result in enhanced drug efficacy, and at the same time minimized undesired side effects. Together with our previous work, we believe that this principle-of-concept is adaptive to build various enzyme-triggered self-assembled materials as smart controlled-release systems capable of site-specific response.

Experimental Section

Material preparation

Protamine sulfate salt from salmon, trypsin from bovine pancreas, and trisodium salt of 8-hydroxypyrene-1,3,6-trisulfonic acid (HPTS) were purchased from Sigma-Aldrich. Doxorubicin hydrochloride (DOX), glucose oxidase (GOx), proteinase K, α -chymotrypsin, and fluorescein sodium were purchased from Aladdin. Alkaline phosphatase (CIAP) and exonuclease I (Exo I) were purchased from Takara. Arginine was purchased from Bio Basic Inc. and 4-phenol-sulfonic sodium was purchased from Acros. All of these were used without further purification. *p*-Sulfonatocalix[4]arene (SC4A) and 5,11,17,23-tetrakisulfonato-25,26,27,28-tetrakis(ethyl)-calix[4]arene (ethyl-modified SC4A at OH groups) were synthesized and purified according to the procedures reported previously^[53,54] and identified using ¹H NMR spectroscopy in D₂O, performed on a Varian 300 spectrometer, and elemental analysis, performed on a Perkin-Elmer 2400C instrument. SC4A-protamine vesicle was prepared by a simple mixture of SC4A and stable protamine in aqueous solution and it would achieve balance over 1 h. Trypsin-responsive disassembly of the SC4A-protamine vesicle in water would lead to form some precipitates, and related experiments were performed after removing the precipitates.

DOX-, HPTS-, and fluorescein-loaded vesicles: DOX-, HPTS-, and fluorescein-loaded vesicles were prepared as follows: A certain amount of DOX, HPTS, or fluorescein was added to a solution containing protamine, and then SC4A and water were added until the volume of the solution reached 25 mL. The ultimate concentrations of HPTS, protamine, and SC4A for HPTS-loaded vesicles in controlled-release experiments were 0.01 mM, 50 $\mu\text{g mL}^{-1}$, and 0.02 mM, respectively, and the ultimate concentration of HPTS is 0.1 mM for HPTS-loaded vesicles in cell experiments. The ultimate concentrations of DOX, protamine, and SC4A for DOX-loaded vesicles in UV/Vis experiments were 0.01 mM, 50 $\mu\text{g mL}^{-1}$, and 0.02 mM, respectively, and the ultimate concentration of DOX is 0.002 mM for DOX-loaded vesicles in cell experiments. The ultimate concentrations of fluorescein, protamine, and SC4A for fluorescein-loaded vesicles in fluorescence imaging were 0.3, 5 mg mL^{-1} , and 2 mM, respectively. One hour later, the prepared DOX-, HPTS-, and fluorescein-loaded vesicles were purified by dialysis (molecular weight cut-off=3500) in distilled water several times until the water outside the dialysis tube exhibited negligible DOX, HPTS, or fluorescein fluorescence. The DOX loading efficiency was calculated with the following Equation:

$$\text{Loading efficiency (\%)} = (m_{\text{DOX-loaded}}/m_{\text{NPs}}) \times 100$$

in which, $m_{\text{DOX-loaded}}$ and m_{NPs} are mass of DOX encapsulated in vesicles and mass of DOX-loaded vesicles, respectively. The mass of DOX was measured by a UV spectrophotometer at 490 nm and calculated as relative to a standard calibration curve in the concentrations from 3.82 to 22.92 $\mu\text{g mL}^{-1}$ in water.

UV/Vis spectra

UV/Vis spectra and the optical transmittance of the aqueous solution were measured in a quartz cell (light path 10 mm) on a Shimadzu UV-3600 spectrophotometer equipped with a PTC-348WI temperature controller.

Fluorescence spectra

Steady-state fluorescence spectra were recorded in a conventional quartz cell (light path 10 mm) on a Varian Cary Eclipse equipped with a Varian Cary single-cell Peltier accessory to control temperature ($\lambda_{\text{ex}}=339.0$ nm, bandwidth (ex) 2.5 nm, bandwidth (em) 5.0 nm).

High-resolution TEM and SEM experiments

High-resolution TEM images were acquired using a Tecnai 20 high-resolution transmission electron microscope operating at an accelerating voltage of 200 keV. The sample for high-resolution TEM measurements was prepared by dropping the solution onto a copper grid. The grid was then air-dried. SEM images were recorded on a Hitachi S-3500N scanning electron microscope. The sample for SEM measurements was prepared by dropping the solution onto a coverslip, followed by evaporating the liquid in air.

Cryo-TEM experiments

Cryo-TEM was performed on an FEI Tecnai 20. A drop of solution was dropped onto a copper grid coated with a holey carbon support film. After 15 s, the water was removed by paper. The copper grid was immersed into liquid C_2H_6 immediately and then transferred into liquid nitrogen for further observation.

DLS measurements

The sample solution for DLS measurements was prepared by filtering solution through a 450 nm Millipore filter into a clean scintillation vial. The samples were examined on a laser light-scattering spectrometer (BI-200SM) equipped with a digital correlator (Turbo-Corr) at 636 nm at a scattering angle of 90° .

Zeta potential measurement

Zeta potential of the SC4A-protamine vesicle was measured by ZetaPALS + BI-90 instrument (Brookhaven Co. USA).

Cell experiments

NIT-1 cells (pancreatic islet beta cells in mice) and PANC-1 cells (pancreatic carcinoma cells in human) were seeded in clear 24-well plates at a density of 2×10^4 cells per well in 1000 μL of complete RPMI 1640 and 10% fetal calf serum (FCS) and grown for 24 h with 5% CO_2 at 37°C . HepG-2 cells (hepatic carcinoma cells in human) were seeded in a clear 24-well plate at a density of 2×10^4 cells per well in 1000 μL of complete Dulbecco's Modified Eagle Medium (DMEM) and 10% fetal calf serum (FCS) and grown for 24 h with 5% CO_2 at 37°C . NIT-1 cells were subsequently incubated with and without the SC4A-protamine vesicle. HepG-2 cells and PANC-1 cells were subsequently incubated with and without DOX and DOX-loaded vesicle. After another 24 h of incubation, the number of living cells in every group was measured. The number of living cells is expressed as the mean \pm standard deviation, and a *t*-test was used for statistical analysis of the data. Differences were considered statistically significant when the *P* value was less than 0.05.

Optical and fluorescence microscopy experiments

PANC-1 cells (pancreatic carcinoma cells in human) were seeded in a clear 24-well plate at a density of 2×10^4 cells per well in complete RPMI 1640 (1000 μL) and 10% fetal calf serum (FCS) and grown for 24 h with 5% CO_2 at 37°C . These cells were subsequent-

ly incubated with HPTS-loaded vesicles. After another 24 h of incubation, the optical and fluorescence microscopic images for these cells were performed on an OLYMPUS BX51 fluorescence microscope (Anaheim, USA) with a 100 W DC mercury lamp for excitation and a Mc MP5 color CCD camera for photograph collection.

Fluorescence imaging in mice

Male BALB/C-nu mice with weights of (19.5 ± 0.5) g were purchased from Beijing HFK Bioscience Co., Ltd. and used in this study. All of the animal studies were approved and in accordance with China's National Code of Animal Care for Scientific Experimentation. The mice were intraperitoneally injected with 100 μL of the fluorescein-loaded vesicles in pancreatic tissue. Similar experiments were conducted with the bare fluorescein at the same fluorescein concentration. The mice were anesthetized and the time-dependent biodistribution of fluorescein in the mice was imaged using a Bethold NightOWL LB 983 in vivo Imaging System (Bad Wildbad, Germany). Light with a central wavelength of 480 nm was selected as the excitation source. In vivo spectral imaging of 520 nm was conducted, with a constant exposure time for each image frame. Autofluorescence was removed by the blank control experiments of the mice injected with 100 μL of normal saline following the same procedure. Scans were carried out at 3 min post-injection. The images were recorded with a built-in CCD camera.

Acknowledgements

We thank the 973 Program (2011CB932502) and NSFC (20932004 and 21172119) for financial support. We would also like to thank group member Yi-Xuan Wang for his assistance in the preparation of this manuscript, and thank Jia-Tong Chen (College of Life Sciences, Nankai University) and Zhong-Hua Li (College of Pharmacy, Nankai University) for their assistance in biological experiments.

Keywords: aggregation • calixarenes • enzymes • host-guest systems • vesicles

- [1] X. Zhang, S. Rehm, M. M. Safont-Sempere, F. Würthner, *Nat. Chem.* **2009**, *1*, 623–629.
- [2] P. F. Kiser, G. Wilson, D. Needham, *Nature* **1998**, *394*, 459–462.
- [3] J. C. M. van Hest, *Nature* **2009**, *461*, 45–47.
- [4] D. M. Vriezema, M. C. Aragonès, J. A. A. W. Elemans, J. J. L. M. Cornelissen, A. E. Rowan, R. J. M. Nolte, *Chem. Rev.* **2005**, *105*, 1445–1489.
- [5] G. Fuks, R. M. Talom, F. Gauffre, *Chem. Soc. Rev.* **2011**, *40*, 2475–2493.
- [6] X. Guo, F. C. Szoka Jr, *Acc. Chem. Res.* **2003**, *36*, 335–341.
- [7] T. Kunitake, *Angew. Chem.* **1992**, *104*, 692–710; *Angew. Chem. Int. Ed. Engl.* **1992**, *31*, 709–726.
- [8] Z. Yang, G. Liang, B. Xu, *Acc. Chem. Res.* **2008**, *41*, 315–326.
- [9] S. Samantaray, R. Sharma, T. K. Chattopadhyaya, S. D. Gupta, R. Ralhan, *J. Cancer Res. Clin. Oncol.* **2004**, *130*, 37–44.
- [10] A. Spaltenstein, W. M. Kamierski, J. F. Miller, V. Samano, *Curr. Top. Med. Chem.* **2005**, *5*, 1589–1607.
- [11] T. Guo, D. W. Hobbs, *Curr. Med. Chem.* **2006**, *13*, 1811–1829.
- [12] S. H. Um, J. B. Lee, N. Park, S. Y. Kwon, C. C. Umbach, D. Luo, *Nat. Mater.* **2006**, *5*, 797–801.
- [13] R. J. Williams, A. M. Smith, R. Collins, N. Hodson, A. K. Das, R. V. Ulijn, *Nat. Nanotechnol.* **2009**, *4*, 19–24.
- [14] J. Hu, G. Zhang, S. Liu, *Chem. Soc. Rev.* **2012**, *41*, 5933–5949.
- [15] R. V. Ulijn, *J. Mater. Chem.* **2006**, *16*, 2217–2225.
- [16] P. D. Thornton, R. J. Mart, R. V. Ulijn, *Adv. Mater.* **2007**, *19*, 1252–1256.
- [17] M. P. Lutolf, J. A. Hubbell, *Nat. Biotechnol.* **2005**, *23*, 47–55.

- [18] M. A. Azagarsamy, P. Sockalingam, S. Thayumanavan, *J. Am. Chem. Soc.* **2009**, *131*, 14184–14185.
- [19] K. R. Raghupathi, M. A. Azagarsamy, S. Thayumanavan, *Chem. Eur. J.* **2011**, *17*, 11752–11760.
- [20] Y. Wang, H. Xu, X. Zhang, *Adv. Mater.* **2009**, *21*, 2849–2864.
- [21] X. Zhang, C. Wang, *Chem. Soc. Rev.* **2011**, *40*, 94–101.
- [22] C. Wang, Z. Wang, X. Zhang, *Acc. Chem. Res.* **2012**, *45*, 608–618.
- [23] C. Wang, Q. Chen, Z. Wang, X. Zhang, *Angew. Chem.* **2010**, *122*, 8794–8797; *Angew. Chem. Int. Ed.* **2010**, *49*, 8612–8615.
- [24] Y. Xing, C. Wang, P. Han, Z. Wang, X. Zhang, *Langmuir* **2012**, *28*, 6032–6036.
- [25] C. Wang, Y. Kang, K. Liu, Z. Li, Z. Wang, X. Zhang, *Polym. Chem.* **2012**, *3*, 3056–3059.
- [26] Y. Kang, C. Wang, K. Liu, Z. Wang, X. Zhang, *Langmuir* **2012**, *28*, 14562–14566.
- [27] E. N. Savariar, S. Ghosh, D. C. González, S. Thayumanavan, *J. Am. Chem. Soc.* **2008**, *130*, 5416–5417.
- [28] D. Guo, K. Wang, Y. Wang, Y. Liu, *J. Am. Chem. Soc.* **2012**, *134*, 10244–10250.
- [29] K. Kim, N. Selvapalam, Y. H. Ko, K. M. Park, D. Kim, J. Kim, *Chem. Soc. Rev.* **2007**, *36*, 267–279.
- [30] D. Guo, Y. Liu, *Chem. Soc. Rev.* **2012**, *41*, 5907–5921.
- [31] Y. Liu, Y. Chen, *Acc. Chem. Res.* **2006**, *39*, 681–691.
- [32] A. Harada, Y. Takashima, H. Yamaguchi, *Chem. Soc. Rev.* **2009**, *38*, 875–882.
- [33] R. Sun, C. Xue, X. Ma, M. Gao, H. Tian, Q. Li, *J. Am. Chem. Soc.* **2013**, *135*, 5990–5993.
- [34] F. Perret, A. N. Lazar, A. W. Coleman, *Chem. Commun.* **2006**, *42*, 2425–2438.
- [35] F. Perret, A. W. Coleman, *Chem. Commun.* **2011**, *47*, 7303–7319.
- [36] V. D. Uzunova, C. Cullinane, K. Brix, W. M. Nau, A. I. Day, *Org. Biomol. Chem.* **2010**, *8*, 2037–2042.
- [37] K. Uekama, F. Hirayama, T. Irie, *Chem. Rev.* **1998**, *98*, 2045–2076.
- [38] Y. J. Jeon, P. K. Bharadwaj, S. W. Choi, J. W. Lee, K. Kim, *Angew. Chem.* **2002**, *114*, 4654–4656; *Angew. Chem. Int. Ed.* **2002**, *41*, 4474–4476.
- [39] Q. Yan, J. Yuan, Z. Cai, Y. Xin, Y. Kang, Y. Yin, *J. Am. Chem. Soc.* **2010**, *132*, 9268–9270.
- [40] K. Wang, D. Guo, Y. Liu, *Chem. Eur. J.* **2010**, *16*, 8006–8011.
- [41] K. Wang, D. Guo, X. Wang, Y. Liu, *ACS Nano* **2011**, *5*, 2880–2894.
- [42] K. Wang, D. Guo, Y. Liu, *Chem. Eur. J.* **2012**, *18*, 8758–8764.
- [43] N. Basilio, L. García-Río, *Chem. Eur. J.* **2009**, *15*, 9315–9319.
- [44] V. Francisco, N. Basilio, L. García-Río, J. R. Leis, E. F. Maques, C. Vázquez-Vázquez, *Chem. Commun.* **2010**, *46*, 6551–6553.
- [45] N. Basilio, M. Martín-Pastor, L. García-Río, *Langmuir* **2012**, *28*, 6561–6568.
- [46] P. K. Buamah, A. W. Skillen, *Clin. Chem.* **1985**, *31*, 876–877.
- [47] A. F. Paszcuk, N. L. M. Quintão, E. S. Fernandes, L. Juliano, K. Chapman, P. Andrade-Gordon, M. M. Campos, N. Vergnolle, J. B. Calixto, *Eur. J. Pharmacol.* **2008**, *581*, 204–215.
- [48] Z. Lu, F. Wu, X. Miao, W. Yu, *Clin. J. Med. Offic.* **2008**, *36*, 488–490.
- [49] D. Guo, K. Wang, Y. Liu, *J. Inclusion Phenom. Macrocyclic Chem.* **2008**, *62*, 1–21.
- [50] R. E. McGovern, H. Fernandes, A. R. Khan, N. P. Power, P. B. Crowley, *Nat. Chem.* **2012**, *4*, 527–533.
- [51] M. Rehm, M. Frank, J. Schatz, *Tetrahedron Lett.* **2009**, *50*, 93–96.
- [52] M. Lee, S.-J. Lee, L.-H. Jiang, *J. Am. Chem. Soc.* **2004**, *126*, 12724–12725.
- [53] G. Arena, A. Contino, G. G. Lombardo, D. Sciotto, *Thermochim. Acta* **1995**, *264*, 1–11.
- [54] S. Shinkai, S. Mori, H. Koreishi, T. Tsubaki, O. Manabe, *J. Am. Chem. Soc.* **1986**, *108*, 2409–2416.

Received: October 10, 2013

Revised: December 18, 2013

Published online on March 5, 2014